A Trapped Degenerate Mode Magnetic Acoustic Resonator

<u>Barry J Gallacher</u>[*], Jim Burdess[*], Zhongxu Hu[*], Harriet Grigg[*], Carl Dale[**], Chen Fu[**], Neil Keegan[**], John Hedley[*] and Julia Spoors[**]

[*]*School of Engineering, Newcastle University, Newcastle, UK*   [**]*Institute of Cellular Medicine, Newcastle University, Newcastle, UK*

<u>*Summary*</u>. Trapped Degenerate resonators offer significant advantages for several sensing applications including mass detection and gyroscopic sensors. In this paper the trapped degenerate modes of vibration produce in-plane displacements at the surface of the resonator. Out of plane motion of the surface is relatively small and can be reduced through modification of the design thus making this device type ideal for sensing under fluid where out of plane displacement would result in significant or total quenching of the required vibration. Excitation of the pair of degenerate modes is performed through magnetic acoustic coupling using a superposition of a time harmonic axisymmetric magnetic field with static cyclically symmetric magnetic field. The cyclic order of the magnetic field determines the mode order of the resonant response. The experimental modeshape has been mapped using 3D laser vibrometry and compares favourably with full elastodynamic finite element modelling.

Introduction

Mass sensing under liquid presents a significant challenge to mechanical resonators. It has been reported, [1], that out of plane surface displacement causes severe damping rendering resonant based mass detection impossible. In this study the resonator geometry is configured to support **trapped degenerate** modes with in-surface shear vibrations at its surface. The resonator will be expected to possess an inherently high quality factor and permit mass detection under liquid through differential measurement of a pair degenerate resonant frequencies [2]. Mass sensing using through the absolute frequency shift of a single mode of vibration of a magnetic acoustic resonator as in [4-9] is susceptible to any environmental effect that can cause changes to the resonant frequency of that single mode. An alternative approach largely insensitive to the unwanted causes of frequency shift is made possible through using well-known degenerate modal properties of cyclically symmetric structures [10]. Independent cyclic modes which vary circumferentially as $\sin(n\theta)$ and $\cos(n\theta)$, $n \neq 0$, share a common resonant frequency ω_n. When mass is added to these resonators, in a way which disrupts this symmetry, then the degeneracy is broken and the single resonant frequency 'splits' to yield two, close, resonant frequencies ω_{n1} and ω_{n2}. This frequency split is used to record the added mass. Common mode effects e.g. temperature and liquid effects are removed by this differential measurement [3].
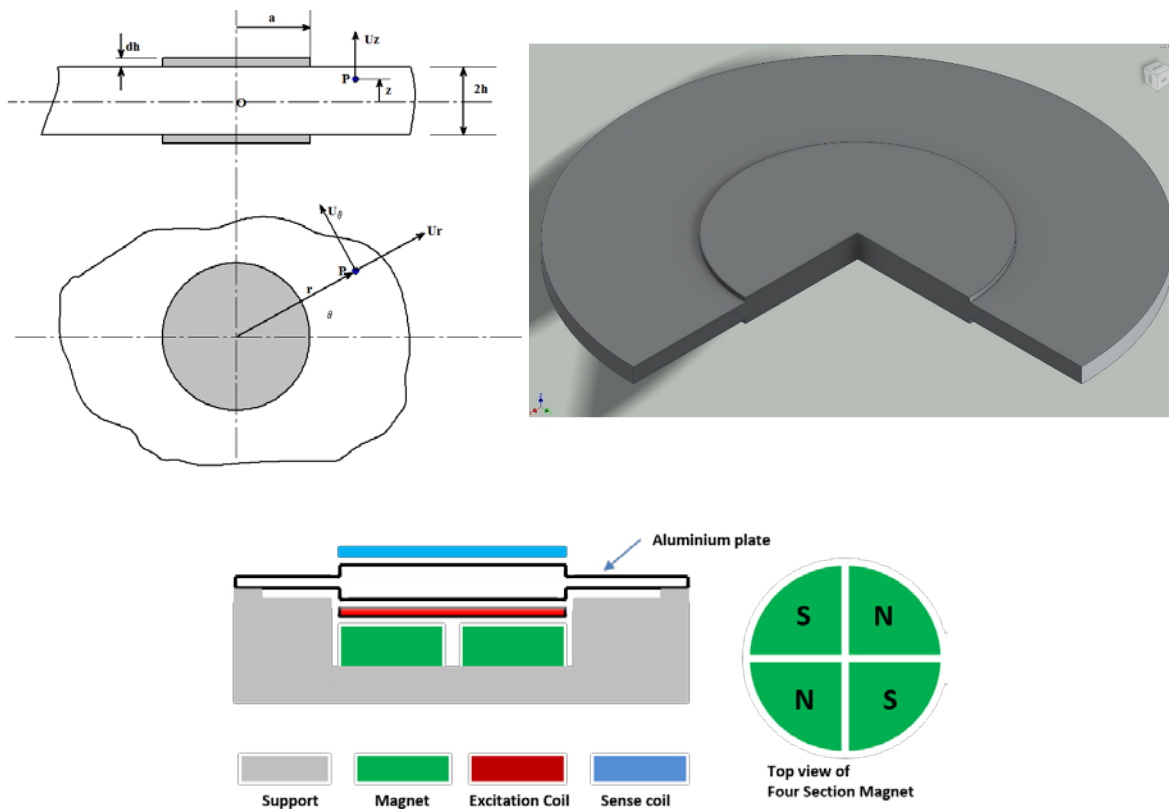
Fig.1 System description

Description of the system

The resonator is formed in aluminium plate with a central circular mesa machined symmetrically onto the top and bottom surfaces. The dispersion relation for an infinite aluminium plate can be plotted for the two thicknesses corresponding to the plate with and without the mesa. Figure 2 shows the dispersion plots. The Bechmann numbers k_{B1} and k_{B2} define the frequencies in the plate and mesa respectively corresponding to case where the radial wave number ξ is zero [11]. Furthermore, the Bechmann numbers define the cut-off frequencies below which the radial wave number ξ becomes imaginary. By selecting a frequency parameter k_{BC} such that $k_{B1} < k_{BC} < k_{B2}$ the wave in the region defined by the mesa will be propagating whilst the wave outside the mesa will be evanescent. The mode is localised. The resonant frequency ω_B is related to the frequency parameter by k_B by

$$k_B{}^2 = \omega_B{}^2 h^2 \frac{\rho}{\mu}$$

where ρ and μ are the mass density and shear modulus for the Aluminium.

The trapped and quasi-trapped modes are expected to have a resonant frequency ω_{BC} with
$\omega_{B1} < \omega_{BC} < \omega_{B2}$.
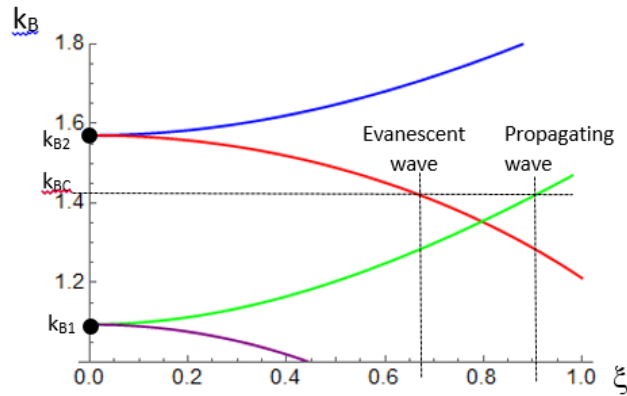
Fig.2 Dispersion plot for layered plate

Electromagnetic excitation of cyclically symmetric in-plane modes

Electromagnetic excitation of acoustic waves was first demonstrated in the late 1960's [12] and has been explored in recent years as a means of realising high quality factor resonators for mass detection [5-9]. Figure 1 illustrates the device, the excitation and detection coils. The mechanical resonator is an aluminium plate with a central mesa machined symmetrically on its top and bottom surfaces. A sinusoidally time varying current is driven through the pancake coil situated below the central mesa. Directly below the excitation pancake coil is a cyclically symmetric arrangement of permanent magnets.

.
As the pancake coil is axisymmetric to first order, the induced Eddy current in the aluminium plate will also be axisymmetric. The Eddy current is confined within the skin depth near the bottom surface of the Aluminium plate. The Lorentz interaction of this Eddy current with the permanent magnetic arrangement results in a circumferentially distributed time varying force that can be used for resonant excitation of degenerate modes. The nature of the forcing from the combination of static and time varying magnetic fields is conveniently described by the Maxwell stress [16]. With reference to figure 1, $(\hat{r}, \hat{\theta}, \hat{z})$ defines unit vectors in the radial, tangential, and out of plane directions. The displacement vector of an arbitrary point P is $\left(U_r \hat{r}, U_\theta \hat{\theta}, U_z \hat{z}\right)$. The air gap between the aluminium plate is very small compared to the in-plane dimensions of the plate. As a result, the cyclic arrangement of permanent magnets creates a magnetic flux density in the aluminium plate which may be approximated to

$$\underline{B}^{(p)} = B_z^{(p)} \cos(n\theta)\, \hat{\underline{z}}\,.$$

For the case considered $n=2$. Fourier decomposition of the cyclic arrangement of permanent magnets will also contain other harmonics. These additional harmonics are small relative to the fundamental component $n=2$ and are consequently neglected. The magnetic flux density generated by the pancake coil can be described by

$$\underline{B}^{(c)} = \left(\tilde{B}_r^{(c)} \hat{\underline{r}} + \tilde{B}_z^{(c)} \hat{\underline{z}}\right) e^{i\omega t}$$

The magnetic flux density of the coil is orders of magnitude smaller than that of the permanent magnetic. A small parameter ϵ may then be defined as

$$\epsilon = \frac{\tilde{B}_r^{(c)}}{B_z^{(p)}} \text{ where } \epsilon \ll 1.$$

Similarly, the radial component of the field from the coil dominates then the approximation $\tilde{B}_z^{(c)} = \epsilon \tilde{B}_r^{(c)}$ can be made yielding

$$\underline{B}^{(c)} = \left(\epsilon B_r^{(c)} \hat{\underline{r}} + \epsilon^2 B_z^{(c)} \hat{\underline{z}}\right) e^{i\omega t}$$

The total magnetic flux density is

$$\underline{B} = \underline{B}^{(c)} + \underline{B}^{(p)}$$

The Maxwell stress components acting in the Aluminium plate due to the total magnetic flux density can be determined from

$$\sigma_{ij} = \frac{1}{\mu_0}\left(B_i B_j - \frac{1}{2}\delta_{ij}B^2\right).$$

The stress components acting within the plate are therefore

$$\sigma_{rz} = \frac{1}{\mu_0}\left(\epsilon B_r^{(c)} B_z^{(p)} \cos(n\theta) e^{i\omega t} + O(\epsilon^3)\right)$$

$$\sigma_{zz} = -\frac{1}{2\mu_0}\left(B_z^{(p)^2} \cos^2(n\theta) + O(\epsilon^2)\right)$$

$$\sigma_{rr} = O(\epsilon^2)$$

Resonant excitation of the SH modes of cyclic order n is made possible through the shear stress σ_{rz}. As the σ_{rz} stress distribution is confined to the within skin depth from the bottom surface, the harmonic forcing will preferentially excite in-plane shear modes which are antisymmetric through the thickness. However, it should be noted that the generalised force pertaining to the symmetric modes is not zero.

Numerically calculated modeshape

The frequency response of the system was calculated using COMSOL finite element analysis software in order to provide a comparison with the experimental results. A full elastic model was used. Figure 3 shows the displacement components of the mode corresponding to the experimentally characterized response. Note that the numerical model is perfectly axisymmetric and as a result the cyclic modes are degenerate.
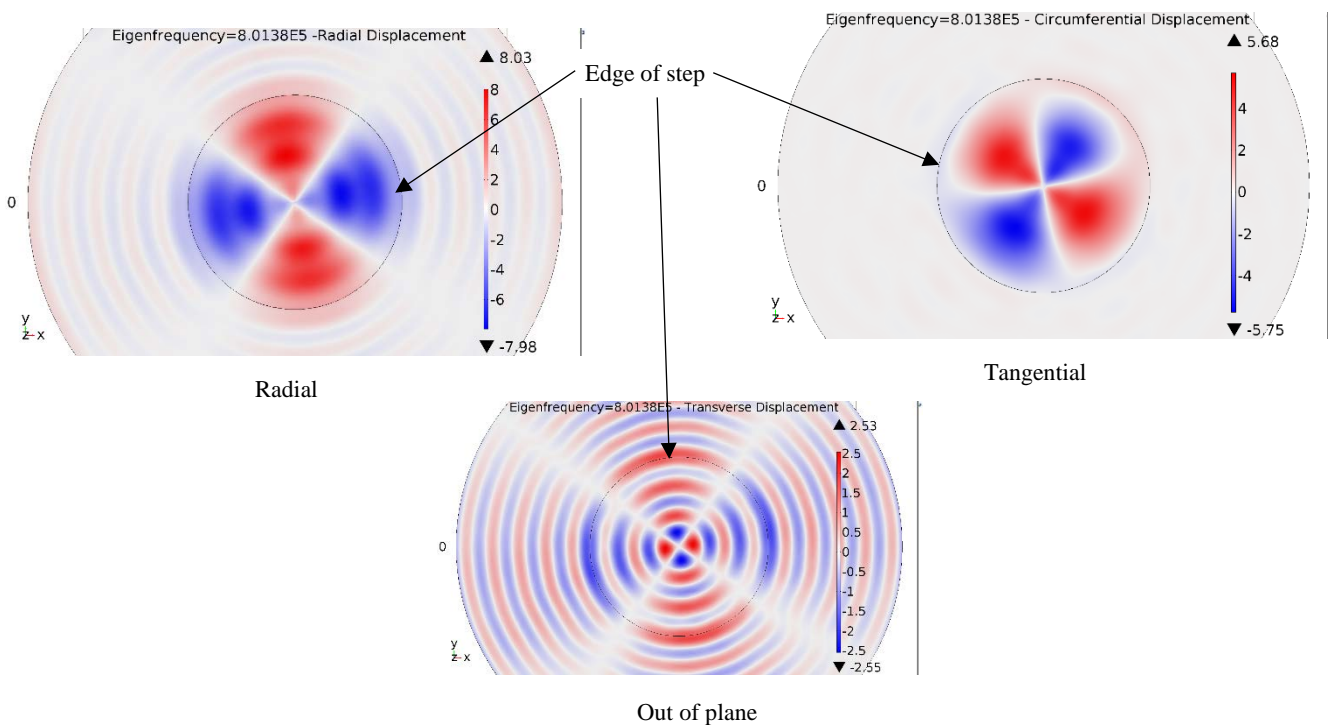
Fig.3 Modeshape displacement components determined through finite element modelling

Experimental frequency response and modeshape

The frequency response was measured both electromagnetically and by laser vibrometry. The frequency range of interest was determined by the Bechmann numbers. Figure 4 shows the measure frequency response for this range. All the responses shown are of cyclic order $n=2$. Structural imperfections breaking the conditions for ideal degeneracy will be inevitable. This causes a frequency split between the modes within each pair which is evident in the figure. The response of both largest amplitude and Q-factor was exhibited by the mode pair with the average resonant frequency of $\omega_n=$ 834.5 KHz. Due to its relatively high Q factor (30000) this mode pair is most likely the quasi-trapped mode. Laser vibrometry using the Polytec MSA 100 3D was performed to measure the inplane and out of plane displacement displacement of the resonant response. Figure 5 shows the measured displacement components. Note that the radial displacement component is shown as a magnitude plot.
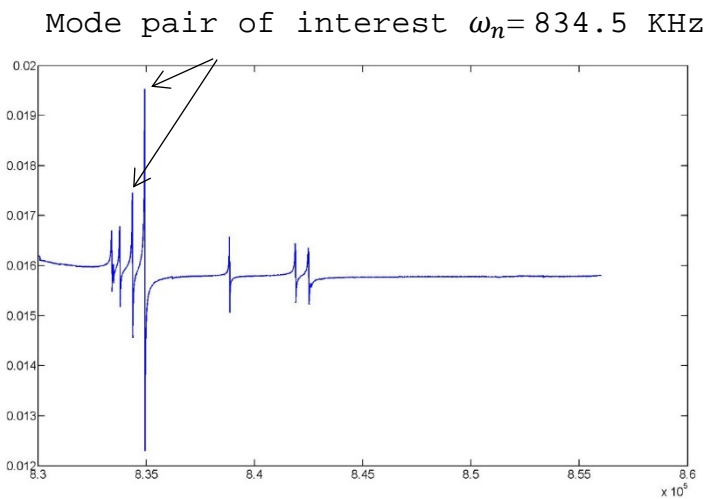
Mode pair of interest $\omega_n=$ 834.5 KHz

Fig.4 Modeshape displacement components determined through finite element modelling

Radial

Tangential

Out of plane
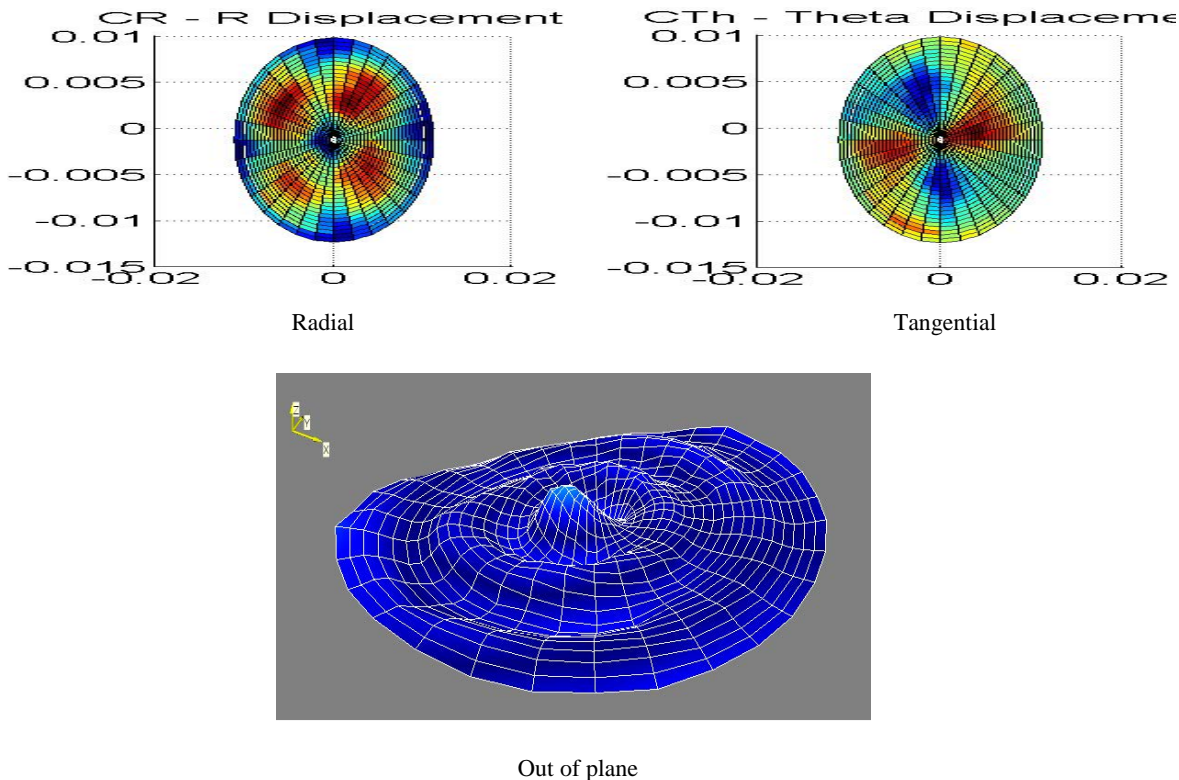
Fig.5 Experimental modeshape displacement components measured by 3D laser vibrometry

Experimental configuration

The complete experimental setup is shown in figure 4. The EMF *V* generated in the aluminium plate is a consequence of two effects and is described by

$$V = -\oint \frac{dA}{dt} . \underline{dl} + \oint (\underline{v} \, x \, \underline{B}) . \underline{dl}$$

The time dependent vector potential $\underline{A} = A_\theta (r, z) e^{i\omega t} \hat{\underline{\theta}}$ generated by the excitation coil generates an EMF in the aluminium plate which is independent of the vibration. Detection of the motional EMF from the $\underline{v} \, x \, \underline{B}$ component, where $\underline{v}$ is the velocity of the plate surface, is through the magnetic field generated by this harmonic motion. Detection of this magnetic field is accomplished through the pair of identical sense coils *S1* and *S2* and follow conventional EMAT principles. Frequency responses test where obtained using a Zurich Instruments HF2LI Lock-in Amplifier.
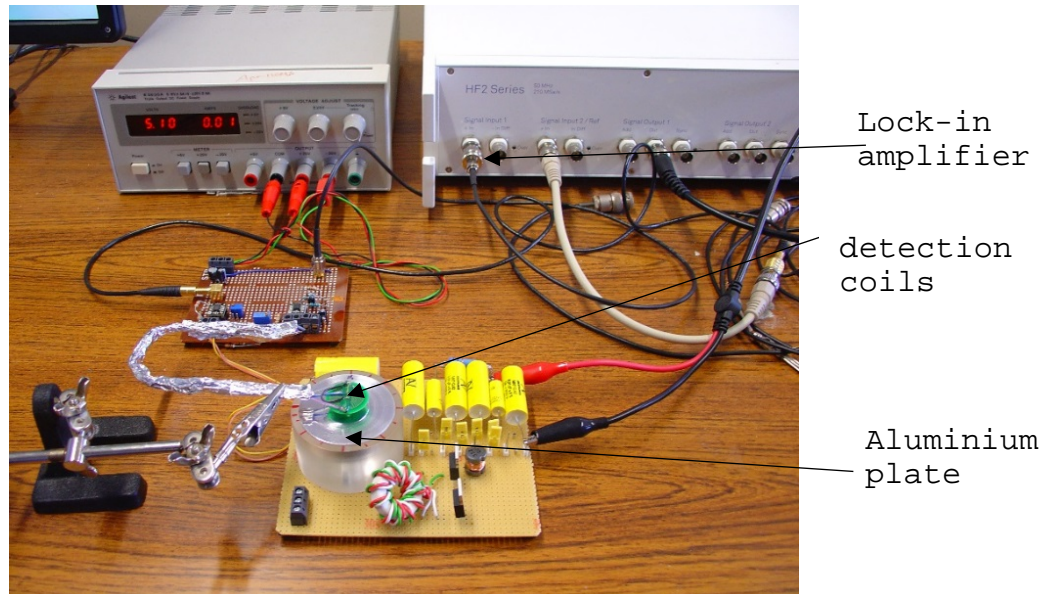
Fig.6 Experimental modeshape displacement components measured by 3D laser vibrometry

Conclusions

Electromagnetic excitation of cyclically symmetric trapped elastic waves resonances have been experimentally demonstrated. The displacement field of the resonant response has been characterised using 3D laser vibrometry and shows that the in-plane surface motion dominates the response. The radial and tangential displacements components of this response are highly localised to the region defined by the mesa. The out of plane displacement does not possess the same degree of localisation. The principal cause of the out of plane displacemnet is coupling casued by the relatively large vertical step due to the mesa. Further work will investigate geometries that minimise the out of plane displacement.

References

[1] K. Lange, et al, Anal. Bioanal. Chem. 391,2008, 1509-1519
[2] A. K. Ismail et-al, J. of Micromechanics and Microengineering, 16, 2006, 1487-1493
[3] A. K. Ismail et-al, J. of Micromechanics and Microengineering, 18(2), 2008
[4] , M. J. Vellekoop, Ultrasonics, 36, 1998, 7-14
[5] A.C. Stephenson and C. R. Lowe, Sensors and Actuators A , 72(1), 1998, 32-37
[6] A.C. Stevenson∗, B. Araya-Kleinsteuber, R.S. Sethi, H.M. Metha, C.R. Lowe, Biosensors and Bioelectronics 20 (2005) 1298–1304
[7] M. K. Kang et-al, Proc. IEEE, International Frequency Control Symposium and Exposition, Dec. 2007, 133-138
[8] Frieder Lucklum, Peter Hauptmann and Nico F de Rooij,Meas. Sci. Technol. **17** (2006) 719–726.
[9] F. Lucklum∗, B. Jakoby Sensors and Actuators A 145–146 (2008) 44–51.
[10] D. L. Thomas, "Dynamics of rotationally periodic structures", *International Journal for Numerical Methods in Engineering*, vol. 14, pp. 81-102, 1979
[11] HF. Tiersten, Thickness vibrations of piezoelectric plates. J. Acoust. Soc. Am. 35: 53-58 1963.
[12] J.J. Quinn, Physics Letters, Vol.25A, No.7, 1967.